Proceedings of the 3rd International Conference on Mechanical Engineering and Mechatronics
Prague, Czech Republic, August 14-15, 2014
Paper No. 140

Simple and Effective OCV Prediction Mechanism for VRLA Battery Systems

Alessandro Mariani*, Thomas Stockley, Kary Thanapalan, Jonathan Williams
Centre for Automotive and Power Systems Engineering (CAPSE)
Faculty of Computing, Engineering & Science
University of South Wales
Pontypridd CF37 1DL, UK
alessandro.mariani@southwales.ac.uk

Peter Stevenson
Yuasa Battery (UK) Ltd
Rassau Industrial Estate
Ebbw Vale NP23 5SD, UK

Abstract -This paper presents an effective technique to monitor and predict the open circuit voltage (OCV) for lead-acid battery cells. The underlying principal of the technique described in this paper employs one simple equation to predict the equilibrated cell voltage after a small rest period. The technique was tested and analyzed using results obtained from experiments conducted at the Yuasa Battery laboratories. Lead-acid battery system analysis was carried out with reference to the standard battery system models available in the literature. The results indicate that by using this technique appreciable benefits can be accrued and it is possible to maintain high standard products in safe operating conditions.

Keywords**:** Lead-acid technology, Cell relaxation, System analysis, Battery system, Predication mechanism.

1. Introduction

The growing demand for green energy and the increasing concern about the global energy shortage have progressively increased the interest in high standard energy sources (Juraschka et al., 2012). The demand for uninterruptible power supply (UPS) systems is growing substantially in parallel with the technical and economic evolution. They are used to protect hardware and electrical equipment, providing emergency power to a load when the input power supply fails (Bitterlin, 2004). This factor has increased the demand of batteries, where the temperatures and the use of products vary widely for different applications (Stephen, 1999). In recent years the consumer needs and product responsibilities have changed. Bank, hospital, telecom, and many other industries have expanded their market, requiring battery devices that can support high rate discharge application in different climate conditions (Mariani et al., 2013).

Although there have been many battery chemistry implementations, to meet the specific needs listed above, the oldest battery chemistries still command a large market share. The lead acid battery may not have the high energy density or fast cycle rates that the lithium and Nickel Metal Hydride (NiMH) technologies possess (Ribeiro et al., 2001) but they are unparalleled in their tolerance for abusive conditions and are low cost (Divya and Ostergaard., 2009). This is most notable in UPS systems where a battery bank can be stored in a remote area, usually an attic or a basement, where conditions can swing between too hot $+40^{o}$ or too cold -20 degree Celsius on a daily basis. The preferred use of lead acid batteries in UPS systems also reflects their low price, with lead acid batteries on average 8.5 times cheaper than lithium technologies (Euro/kWh) (Divya and Ostergaard., 2009). In a system where the batteries are going to be used only in an emergency, low purchase price is essential.

As the batteries are only required in case of an emergency, it is of the utmost importance to ensure that, when called upon, the batteries are in an operational state. To ensure that the cells are in a fully charged state, a monitoring system is used. A coulomb counting method is used for the running state of charge (SoC). However, an accurate initial SoC is required to eliminate errors. There are two established methods for a monitoring system to produce an initial SoC reading. These are: 1) polling of the individual batteries in a pack to measure the internal impedance of each. From the internal impedance the SoC can be derived (Becherif, 2012; Huet, 1998); 2) using the open circuit voltage (OCV)/SoC relationship, where the SoC can be determined by comparing the open circuit voltage to a known OCV/SoC lookup table (Sato and Kawamura., 2002).

A problem with both of these methods is that the batteries need to be in an equilibrated state for accurate measurement, but as the internal resistance is perturbed when the cell enters a state of charge or discharge, the battery voltage will take time to stabilise after the charge or discharge is completed (Floyd, 1994). Work has been conducted to combat the problem of waiting for an equilibrated battery reading by introducing prediction mechanisms. Aylor et al. (1992) proposed a simple OCV prediction mechanism for lead acid batteries, to estimate the 3 hour OCV from a 30 minute open circuit reading. The proposed simple method was not sufficient enough to produce a meaningful result. Therefore, Aylor et al. (1992) conducted further investigation and created a prediction mechanism using asymptotes on a semi log scale. Whilst this method was far more complicated, it worked successfully, providing estimation errors of just 5%.

By contrast Stockley et al. (2013) proved that the simple prediction mechanism introduced by Aylor et al. (1992) can be applied successfully to lithium cells, with the a maximum error of just 0.15%. Furthermore, it noted that this method is difficult to implement for lead acid batteries, because the cells of a lead acid battery have different relaxation curves, whereas lithium cells have a clone like effect between cells of the same type. However, with recent advances in the field of lead acid batteries, it is noted that the cells in a battery have become more unified. This is especially true of the new valve regulated lead acid batteries currently being developed by Yuasa Ltd. Therefore, the work in this paper is conducted to investigate the consequence of applying the simple technique to a set of new lead acid cells. The investigation begins by explaining the cell modeling and its operation in section II. The work then proceeds to the experimental study and proving the simple prediction mechanism is effective and better than the other OCV methods.

2. Cell Modeling and Operation

In the last 50 years battery modeling has been addressed and developed to study electrochemical battery reactions and behavior. This modeling has been used to optimize lead acid cells for different applications (Jackey, 2007) and (Rynkiewicz, 1999). The battery OCV is the difference in potential between the electrodes (Pb and PbO_2) and the concentration of the electrolyte (H_2SO_4), when no load is connected. To have an accurate reading of the OCV the lead acid battery cell needs a few hours to reach a stable equilibrium within its surroundings (Barsali and Ceraolo., 2002). A variety of literature has been published on various aspects of battery cell modeling and operation (Thanapalan et al., 2011) and (Tremblay, 2009), that can be used to simulate and estimate the voltage of a cell from a set of known parameters. Barsani and Ceraolo (2002) defined a dynamic model of lead acid batteries to use in the investigation of their discharge behavior. The general model of a lead acid battery that represents the discharge equivalent network is shown in Fig. 1.

Furthermore, Barsani and Ceraolo (2002) developed their mathematical model as a function of the battery SOC, dependent of the electrolyte concentration, operating temperature and OCV reading. It measures the initial voltage V_o (voltage battery reading in a charged condition), discharged at constant current and recorded the OCV, V_3 and V_4, until the battery reached a stable equilibrium represented in the Fig. 2 as V_1 value.

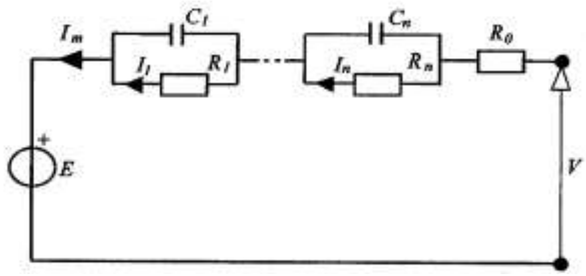

Fig. 1. Lead acid equivalent network for discharge electrochemical reactions (Barsani and Ceraolo., 2002)

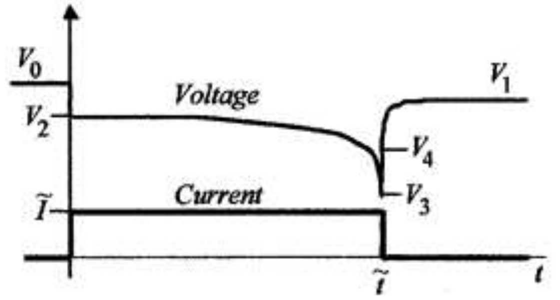

Fig. 2. Typical voltage and current profile for a constant current discharge (Barsani and Ceraolo., 2002)

After trying various methods for the identification of the lead acid battery OCV, it was decided to conduct our investigation based on Aylor's work (1992). With the new lead acid technology, the internal cell equilibrium, at OCV is achieved in the early stages, so the coulometric technique was taken into account in this investigation. The cell voltage can be derived in both the charge and discharge state by using equation (1) and equation (2).

$$V_b^d = E_0 - R.i_b - K\frac{Q}{Q-i_b t}\left(i_b t + i_b^*\right) + A\exp\left(-B.i_b t\right) \tag{1}$$

$$V_b^c = E_0 - R.i_b - K\frac{Q}{i_b t - 0.1Q}.i_b^* - K\frac{Q}{Q-i_b t} + A\exp\left(-B.i_b t\right) \tag{2}$$

Where, V_b^c and V_b^d are the cell voltage during charge and discharge. E_0 is battery constant voltage, R is internal resistance, Q is battery capacity, i_b^* is filtered current and $i_b t$ is actual battery charge. A and B are exponential zone amplitude and time constant inverse respectively.

The equilibrated OCV is given by:

$$V_{oc} = V_{tr} \pm K_v \tag{3}$$

where, V_{OC} is the equilibrated OCV, V_{tr} is the voltage at the time of measurement (30 minutes) and K_v is a constant derived from the equation V_{OC}-V_{tr}.

The cells under study are composed of three main components: 1) Positive electrode made from lead dioxide (PbO_2), 2) Negative electrode made from lead (Pb) in a porous pasted form, and 3) The electrolyte is dilute sulphuric acid (H_2SO_4).

During the discharge process, the electrodes (Pb and PbO_2) break down their equilibrium and an oxidoreduction reaction takes place. The current is transported through the electrolyte, which is available in the plate's pores. In a fully charged condition, the electrolyte is of the same uniform strength (specific gravity) in both the pores of the active material and the separator. During discharge, the chemical reaction between the active material and the electrolyte takes place within the pores of the active material. Fig. 3 identifies the microstructure of the active material under investigation, showing how the pores are arranged across the plate.

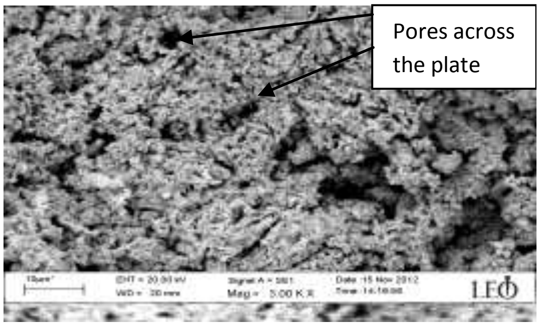

Fig. 3 Scanning Electron Microscope (SEM) active material images.

In a closed loop system, where a load is applied to the cell, the sulphuric acid in the electrolyte of the active material is consumed. This leaves the electrolyte very weak, at a state resembling water, until the cell reaches the discharge cut-off voltage. The cell voltage is related to the strength of the electrolyte in the pores of the active material and very often the cut-off voltage is reached without using the full reserve of strong electrolyte available in the separator. This is especially true in high load conditions. During an open circuit state, the strong electrolyte will gradually diffuse from the separator into the pores of the active material, replacing the very weak electrolyte. This process can be seen by monitoring the OCV, where the voltage of the cell can be seen to increase slowly until after 4 hours voltage appears stable; this is known as the recovery factor. The recovery factor is dependent on the load applied to the cell; a higher load results in a greater difference between the load and equilibrated voltage.

3. Results and Performance Evaluation

The experimental work conducted during this research work was performed on lead acid cells, from valve regulated lead acid (VRLA) batteries, and are the representation of many tests carried out in Yuasa Ltd laboratory. As the work aims to prove that new advances in lead acid cells allow a more simplistic OCV prediction technique, the testing process was carried out on both "standard" and "advanced" cells. Figures 4 and 5 both show a VRLA battery on test and the test setup respectively. As the battery needs to be intact to ensure any generated results are representative of a production VRLA battery, the Silver-silver sulphate reference electrode technique was used. This technique measures the voltage across the ICC (internal cell connection) and the AGM (absorbed glass mat) to measure the voltage of each individual cell and is as unobtrusive as possible because access is gained through the vent valves as shown in Fig. 4. The advantages of the silver-silver sulphate technique over alternative methods are 1) A precisely defined electrode potential. 2) Relatively simple implementation. 3) Availability in a variety of geometries at low cost (Ruetschi, 2003).

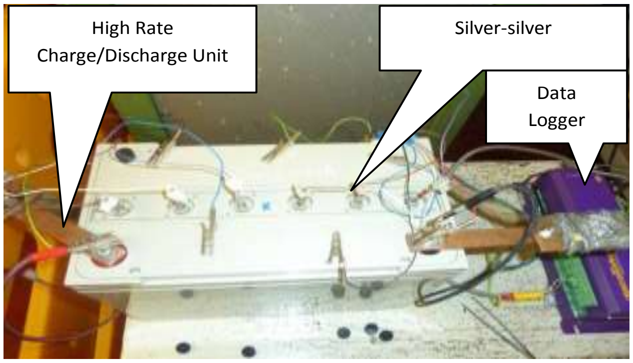

Fig. 4 VRLA battery under test.

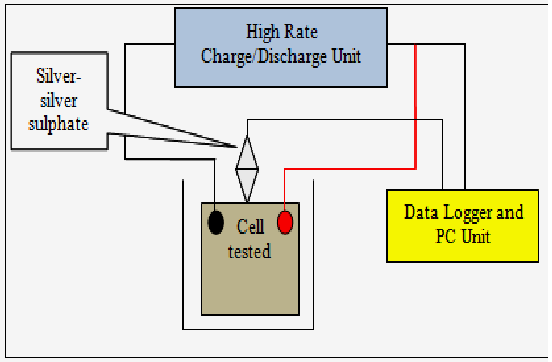

Fig. 5 Block diagram of Experimental setup.

Until now the OCV prediction technique has been unsuccessful for lead acid cells due to the vast differences in cells, even in the same battery. Therefore the first task was to verify that the advanced battery type had a suitable similarity between cells. This was done by a set of capacity tests and relaxation tests. Fig. 6 shows a comparison between 2 advanced cells and 2 standard cells for a 1C discharge. It can be clearly seen, that the results from the advanced product have less variability than the 2 results from the standard product. The standard product actually starts to deviate at 40-50% depth of discharge (DoD), whereas the advanced cells comply with each other until 95-100% DoD. Fig. 6 also highlights the performance enhancement of the advanced cell compared to the standard cell, with the advanced cell voltage higher after 50% DoD.

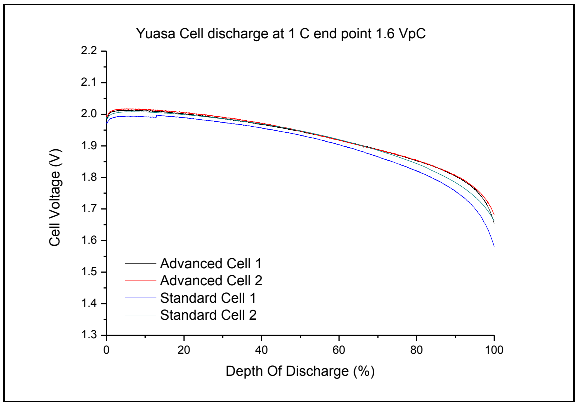

Fig. 6 Behavior comparisons of lead acid cells

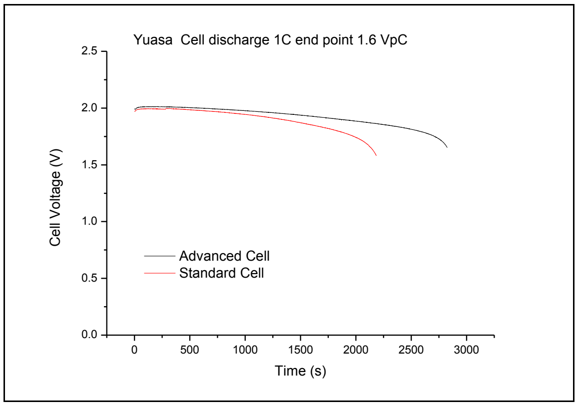

Fig.7 Discharge performance comparisons between advanced and standard cell technology

To further emphasize the superior performance of the advanced cell, the 1C discharges have been plotted against time in Fig. 7. The standard product produced a much lower discharge time of 2319 s, a difference of 509 s. The standard product was made using high density positive active material; very useful for cycling application but less efficient than the new technology product that has greater plate surface area, and porosity. The relaxation test used lead acid cells previously charged for 72 hours at 2.275 volt per cell (v.p.c.), constant power charge technique. The test was carried out in Yuasa Ltd test laboratory using 20^{o} degree Celsius as the ambient temperature operating condition.

The cells were discharged at constant current to 80%, 60%, 40%, and 20% SoC. At the end of each 20% SoC, the cells were given a four hour rest period, where a voltage reading was taken every second. The cells under investigation were discharged at different current rates 0.3C, 1C, and 3C to monitor the variation on relaxation resulting from the increase in load applied on the cell.

To ensure that the results were not discharge rate dependant, the tests were conducted at 0.3C, 1C and 3C for both the standard and advanced products. This was important because in a lead acid cell, the rate of discharge can drastically influence the amount of sulphuric acid consumed in the electrolyte. At low discharge rate, like 0.3C, the active material will be fully utilized by the discharge process, as the cells have enough time to utilize the significant quantity of strong electrolyte from the reservoir of the separator. During high rate discharge application (like 3C rate), the chemical reaction occurs so fast that it does not permit the full utilization of the reservoir of electrolyte contained in the cell separator. Fig. 8 gives an overview of the cell OCV behavior of two standard products following a 1C discharge.

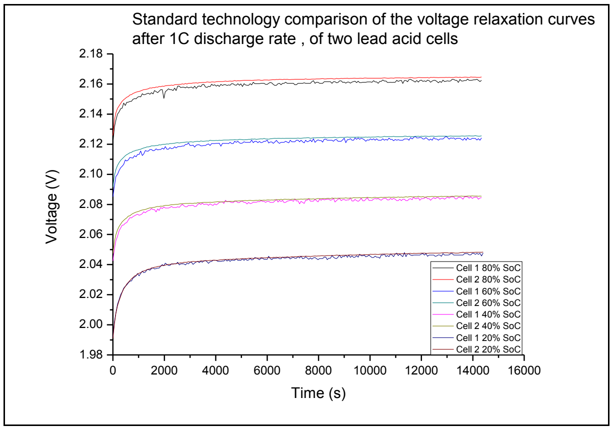

Fig. 8. Comparison of the voltage relaxation curves after 1C discharge, of two lead acid cells

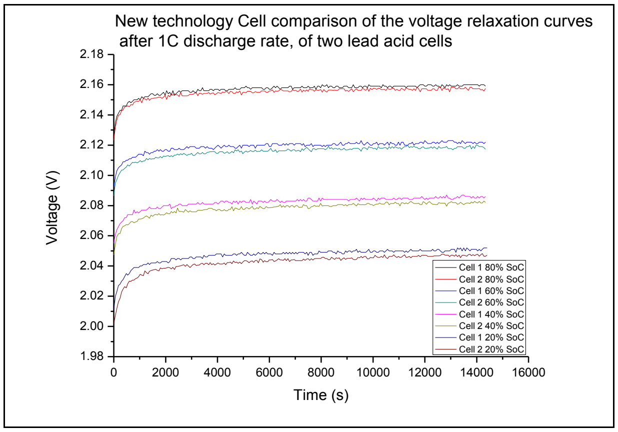

Fig. 9. Comparison of the voltage relaxation curves after 1C discharge, of two advanced technology lead acid cells

Fig. 9 shows the relaxation curves of the advanced technology lead acid cells. As can be seen in Fig. 8, the two cells maintain similar relaxation curves at the different SoC intervals. The advanced type of cell makes use of a low density active material to increase the plate's porosity, and consequently increase the electrolyte available into the pores. This factor increases the discharge efficiency, especially for high load applications. There is a small variation between the 2 cells relaxation curves. This is due to the rate of diffusion of the electrolyte from the separator to the plate's pores, during the open circuit period. This is not a problem because the voltage of the cell will be seen to increase slowly, and stabilize in the next two hours during the OCV period. The results of the standard product OCV test have been compiled into Table 1.The cell voltage (V_{tr}) was measured after 30 minutes at open circuit, however, the true OCV measurement was not stable until the 240 minutes rest interval. For this type of cell the average voltage difference at open circuit from 30 to 240 minutes was 6.45 mV, and was therefore chosen as the K_v constant value. Equation (3) was then used to calculate the predicted OCV after the 240 minutes interval, so that a comparison could be made with the measured (real) OCV after 240 minutes. To aid in this explanation a worked example has been provided below for the 1C relaxation curve at 60% SoC.

$V_{oc} = V_{tr} + K_{v,}\ V_{oc} = 2.118 + 0.00645_{,}\ V_{oc} = 2.1245$ OCV calculated$_{,}$ $V_{real} = 2.1248$ OCV real

The voltage reading error found in this example from calculated and real was -0.0165%. Table 2 contains a comparison of the real and calculated OCV of the investigated cell for all test conditions. The maximum prediction error for the standard product cell was calculated as ± 0.162% and can be seen in Table 2.

Table 1. Voltage measurements from standard product relaxation test.

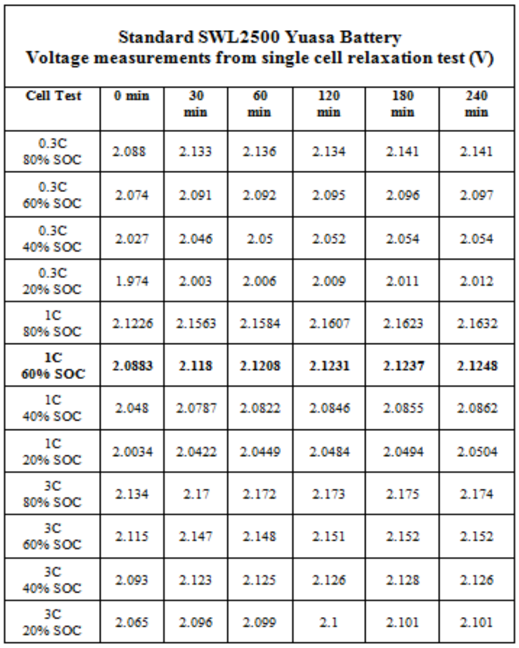

Standard SWL2500 Yuasa Battery
Voltage measurements from single cell relaxation test (V)

Cell Test	**0 min**	**30 min**	**60 min**	**120 min**	**180 min**	**240 min**
0.3C 80% SOC	2.088	2.133	2.136	2.134	2.141	2.141
0.3C 60% SOC	2.074	2.091	2.092	2.095	2.096	2.097
0.3C 40% SOC	2.027	2.046	2.05	2.052	2.054	2.054
0.3C 20% SOC	1.974	2.003	2.006	2.009	2.011	2.012
1C 80% SOC	2.1226	2.1563	2.1584	2.1607	2.1623	2.1632
1C 60% SOC	**2.0883**	**2.118**	**2.1208**	**2.1231**	**2.1237**	**2.1248**
1C 40% SOC	2.048	2.0787	2.0822	2.0846	2.0855	2.0862
1C 20% SOC	2.0034	2.0422	2.0449	2.0484	2.0494	2.0504
3C 80% SOC	2.134	2.17	2.172	2.173	2.175	2.174
3C 60% SOC	2.115	2.147	2.148	2.151	2.152	2.152
3C 40% SOC	2.093	2.123	2.125	2.126	2.128	2.126
3C 20% SOC	2.065	2.096	2.099	2.1	2.101	2.101

Table 2 Comparison of the real and calculated OCV for the standard product.

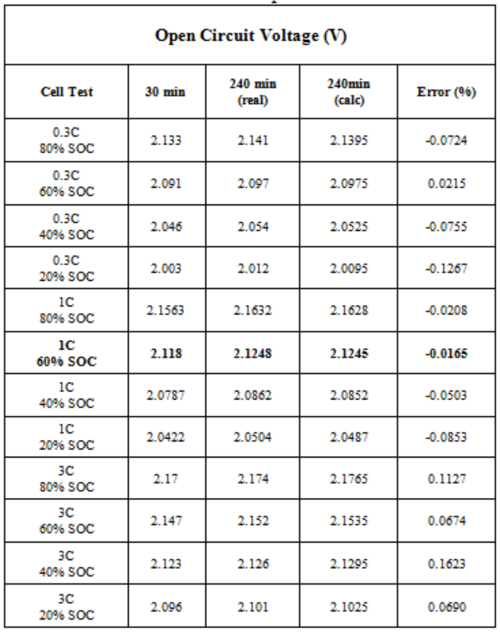

Open Circuit Voltage (V)

Cell Test	**30 min**	**240 min (real)**	**240min (calc)**	**Error (%)**
0.3C 80% SOC	2.133	2.141	2.1395	-0.0724
0.3C 60% SOC	2.091	2.097	2.0975	0.0215
0.3C 40% SOC	2.046	2.054	2.0525	-0.0755
0.3C 20% SOC	2.003	2.012	2.0095	-0.1267
1C 80% SOC	2.1563	2.1632	2.1628	-0.0208
1C 60% SOC	**2.118**	**2.1248**	**2.1245**	**-0.0165**
1C 40% SOC	2.0787	2.0862	2.0852	-0.0503
1C 20% SOC	2.0422	2.0504	2.0487	-0.0853
3C 80% SOC	2.17	2.174	2.1765	0.1127
3C 60% SOC	2.147	2.152	2.1535	0.0674
3C 40% SOC	2.123	2.126	2.1295	0.1623
3C 20% SOC	2.096	2.101	2.1025	0.0690

The OCV prediction technique has also been applied on the advanced technology cell to see how the equation (3) performs on the advanced technology. For the advanced product the K_v constant value chosen was 5.5 mV, because this was the average difference during the test period. The worked example below shows the 0.3C 40% SoC relaxation calculation.

$V_{oc} = V_{tr} + K_v$,$V_{oc} = 2.053V + 0.0055$, $V_{oc} = 2.0585$ OCV calculated, $V_{real} = 2.0590$ OCV real

This worked example, and the results in Table 5, show that the prediction technique can be used on the advanced lead acid product. The worked example produced an error of just -0.024%, with the maximum error for this advanced product at just 0.219%.

Table 3 Voltage measurements from advanced product relaxation test.

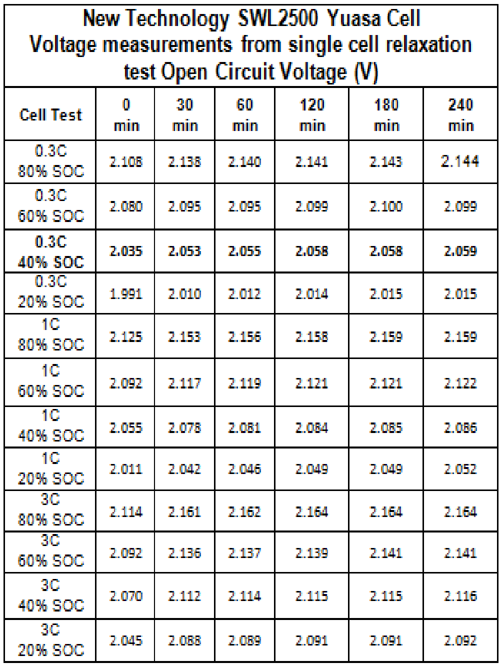

New Technology SWL2500 Yuasa Cell Voltage measurements from single cell relaxation test Open Circuit Voltage (V)						
Cell Test	**0 min**	**30 min**	**60 min**	**120 min**	**180 min**	**240 min**
0.3C 80% SOC	2.108	2.138	2.140	2.141	2.143	2.144
0.3C 60% SOC	2.080	2.095	2.095	2.099	2.100	2.099
0.3C 40% SOC	**2.035**	**2.053**	**2.055**	**2.058**	**2.058**	**2.059**
0.3C 20% SOC	1.991	2.010	2.012	2.014	2.015	2.015
1C 80% SOC	2.125	2.153	2.156	2.158	2.159	2.159
1C 60% SOC	2.092	2.117	2.119	2.121	2.121	2.122
1C 40% SOC	2.055	2.078	2.081	2.084	2.085	2.086
1C 20% SOC	2.011	2.042	2.046	2.049	2.049	2.052
3C 80% SOC	2.114	2.161	2.162	2.164	2.164	2.164
3C 60% SOC	2.092	2.136	2.137	2.139	2.141	2.141
3C 40% SOC	2.070	2.112	2.114	2.115	2.115	2.116
3C 20% SOC	2.045	2.088	2.089	2.091	2.091	2.092

Table 4 Comparison of the real and calculated OCV for the advanced product.

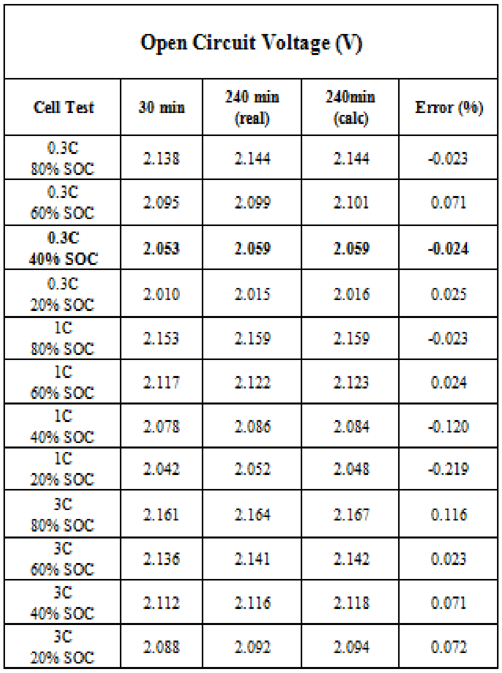

Open Circuit Voltage (V)				
Cell Test	**30 min**	**240 min (real)**	**240min (calc)**	**Error (%)**
0.3C 80% SOC	2.138	2.144	2.144	-0.023
0.3C 60% SOC	2.095	2.099	2.101	0.071
0.3C 40% SOC	**2.053**	**2.059**	**2.059**	**-0.024**
0.3C 20% SOC	2.010	2.015	2.016	0.025
1C 80% SOC	2.153	2.159	2.159	-0.023
1C 60% SOC	2.117	2.122	2.123	0.024
1C 40% SOC	2.078	2.086	2.084	-0.120
1C 20% SOC	2.042	2.052	2.048	-0.219
3C 80% SOC	2.161	2.164	2.167	0.116
3C 60% SOC	2.136	2.141	2.142	0.023
3C 40% SOC	2.112	2.116	2.118	0.071
3C 20% SOC	2.088	2.092	2.094	0.072

4. Discussion and Concluding Remarks

In this paper a simple technique for monitoring and predicting the OCV for lead-acid battery systems are described. By performing various tests using a simple equation it was possible to predict the OCV of a lead-acid cell. The equation was applied to two different rated products: a standard and advanced technology. In both cases the margin of error found from the real OCV and the calculated values was ±0.219%. After a short rest period it was possible to predict the OCV in the lead acid cell successfully. This type of technique gives a greater accuracy of OCV reading when compared with other more complicated methods. Some of which have been described below, in order to show that the simple and effective OCV prediction method described in this paper is good in terms of performance.

Coroban et al. (2007) proposed an online algorithm for prediction of the OCV. The accuracy of this method is dependent on the interval time used during the calculation (sampling time Δt) and on the gain derived experimentally (K factor). The constant K is found using a calibration technique. The technique involves monitoring the battery voltage relaxation curve from the instant a rest period is entered to the time the cell reaches equilibrium. An average error of 1% to 5% was produced by using the methodology provided by Coroban et al. (2007). A statistical analysis method can also be used to estimate the battery OCV as is evident in the work carried out by Snihir et al. (2006). The work by Snihir et al. (2006) monitored the voltage curves following a charge step to specific SoC levels, with a varying current rate. In this case the margin of error obtained when predicting the OCV was 8% to 10%. Bullock et al. (1997) have proposed a model based on polynomial equations to obtain the relationship between acid molarity and OCV. The authors used experimental OCV data acquired during a long self discharge period at different ambient temperatures. This model is capable of predicting the OCV at each temperature condition to within an error of just 2%. Therefore, the simple and effective OCV prediction method, described throughout this research work, provided the OCV with the lowest error rate. This proves that the work in this paper can become a useful tool when used in concomitance with another mathematical method to predict the SoC and state of health (SoH) for electrochemical devices, with more precise results.

References

Aylor J.H., (1992). A battery State of Charge Indicator for Electric Wheelchairs. "Transactions on Industrial Electronics," IEEE, vol.39, issues 5, pp.398-409.

Barsali S., Ceraolo M. (2002). Dynamical Models of Lead-Acid Batteries: Implementation Issues. "Transactions on energy conversion," IEEE, issues 1, pp. 16-23.

Becherif M., Pera M. C., Hissel D. and Jemei S., (2012). Estimation of the Lead-Acid Battery Initial State of Charge with Experimental Validation. "Vehicle Power and Propulsion Conference,"IEEE, pp.469-473.

Bitterlin I. F., (2004). Standby-battery autonomy versus power quality. "J of Power Sources," (136), pp. 351-355.

Bullock K. R., Weeks M. C., Bose C. S. C., Murugesamoorthi K. A., (1997). A predictive model of the reliabilities and the distributions of the acid. "Journal of Power Sources," (64), pp. 139-145.

Coroban V., Boldea I., Blaabjerf F., (2007). A novel on-line state-of-charge estimation algorithm for valve regulated lead-acid batteries used in hybrid electric vehicles. "International Aegean Conference on Electrical Machines and Power Electronics ACEMP,"Bodrum, Turkey, pp.39-46.

Divya K. C. and Ostergaard J., (2009). Battery energy storage technology for power systems—An overview. "Electric Power Systems Research," vol. 79, issues 4, pp.511-520.

Floyd K. D., Noworolski Z., Noworolski J. M., Sokolski W., (1994). Assessment of lead acid battery state of charge by monitor float charging current. "Conference publications,"IEEE, pp. 602-608.

Huet F., (1998). A review of impedance measurements for the determination of the state-of-charge or state-of-health of secondary batteries. "Journal of Power Sources," vol. 70, issue 1, pp. 59-69.

Jackey R. A.,(2007). Simple, Effective Lead-Acid Battery Modelling Process for Electrical System Component Selection. "SAE Paper," 01-0778.

Juraschka H., Thanapalan K., Gusig L., and Premier G., (2012). Optimization strategies for combined heat and power range extended electric vehicles. “In the Proc. of the International Annual Conference of the German Operations Research Society,” Hannover, Germany.

Mariani A., Thanapalan K., Strevenson P., and Williams J.,(2013). Techniques for estimating the VRLA batteries ageing, degradation and failure modes. “In 19th Int. Conf. on Automation and Computing,” UK, pp.43-47.

Ribeiro P. F. et al., (2001). Energy Storage Systems for Advanced Power Applications. “Proceedings of the IEEE,” vol.89, issue 12, pp. 1744-1746.

Ruetschi P., (2003). Silver-silver sulphate reference electrodes for use in lead-acid batteries. “Journal of Power Sources,” (116), pp.53-60.

Rynkiewicz R., (1999). Discharge and charge modeling of lead acid batteries. “In 14th Annual Applied Power Electronics Conference and Exposition IEEE, vol. 2, issue 1, pp.707-710.

Sato S., and Kawamura A., (2002). A New Estimation Method of State of Charge using Terminal Voltage and Internal Resistance for Lead Acid Battery. “Power Conversion Conference,” PCC-Osaka, vol 2, pp. 565-570.

Snihir I., Rey W., Verbitskiy E., Belfadhel-Ayeb A., Nottel P. H. L., (2006). Battery open-circuit voltage estimation by a method of statistical analysis. “Journal of Power Sources,” (159), pp. 1484-1487.

Stephen D., (1999). The K_d Model, Methods of Measurement, and Application of Chemical Reaction Codes. “ Office of Environmental Restoration U.S. Department of Energy,” Washington, DC 20585.

Stockley T., Thanapalan K., Bowkett M., and Williams J., (2013). Development of an OCV Prediction Mechanism for Lithium-Ion Battery System. “In 19th Int. Conf. on Automation and Computing,”, UK, pp. 48-53.

Thanapalan K., Williams J. G., Premier G. C., and Guwy A. J., (2011). Design and Implementation of Renewable Hydrogen Fuel Cell Vehicles.“Renew. Energy Power Qual. J.,” vol. 9, pp.310-315.

Tremblay O., (2009). Experimental Validation of a Battery Dynamic Model for EV Applications, “World Electr. Veh. J.,” vol. 3.